Macromolecules

Article

pubs.acs.org/Macromolecules

Melt Rheology of Ring Polystyrenes with Ultrahigh Purity

Yuya Doi,[†] Kazuki Matsubara,[†] Yutaka Ohta,[†] Tomohiro Nakano,[†] Daisuke Kawaguchi,[‡] Yoshiaki Takahashi,[§] Atsushi Takano,*[,†] and Yushu Matsushita*[,†]

[†]Department of Applied Chemistry, Nagoya University, Furo-cho, Chikusa-ku, Nagoya 464-8603, Japan

[‡]Education Center for Global Leaders in Molecular System for Devices, Kyushu University, Fukuoka 819-0395, Japan

[§]Institute for Materials Chemistry and Engineering, Kyushu University, 6-1, Kasuga-koen, Kasuga, Fukuoka 816-8580, Japan

Supporting Information

ABSTRACT: The melt rheology of highly-purified ring polystyrenes in a wide range of molecular weights (10K ≤ M_w ≤ 240K g/mol) was investigated. All the rings revealed no obvious rubbery plateau and faster terminal relaxation compared to the linear counterparts. The rheological data obtained were compared with some theoretical models such as the Rouse ring model and the lattice-animal model. Moreover, two rheological parameters, zero-shear viscosities η_0 and the steady-state recoverable compliances J_e, were estimated, and their M_w dependence was discussed. From these data analysis, it was found that relaxation mechanisms of ring chains can be divided into three categories depending on their M_w as follows: (i) Smaller rings (M_w ≤ 20K) exhibit faster terminal relaxation than the predicted Rouse rings. This behavior is related to the difference of the local chain conformation from linear chains. (ii) Rings with the moderate molecular weight (40K ≤ M_w ≤ 90K) exhibit dynamic moduli similar to the Rouse ring prediction. (iii) A larger ring (M_w > 90K) also shows deviant behavior from the Rouse chain because its relaxation time is much longer than the Rouse ring prediction and also the lattice-animal model, where some intermolecular interactions are considered to occur.

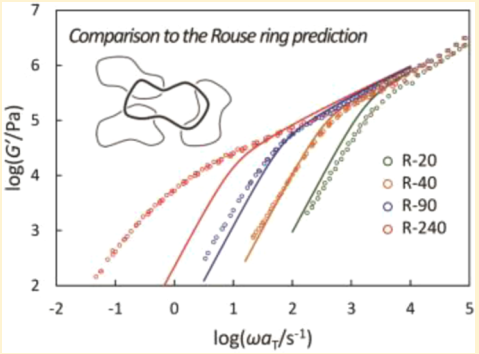

INTRODUCTION

It is well-known that polymer chain architectures significantly affect various physical properties. Especially ring polymers, which are one of the most interesting model polymers, have collected interests of many researchers, as they have no chain ends.[1−5] The chain motion of long flexible linear polymers in concentrated solutions and in the melt is generally understood in the framework of "tube-model" theory with several extensions.[6−9] This model originally assumed that the entangled long linear chains were placed in fixed uncrossable "tubes" and only allowed to move diffusively along their tubes. This motion is called "reptation", and their entanglement relaxation is known to originate from their chain ends. The tube model concept was also applied to the entangled branched polymers,[6−9] although the simple reptation can never occur owing to the existence of the branch points. As the simplest example, the chain motion of star polymers can be described well by introducing the arm retraction process into the tube model. To the contrary, a simple application of the tube-model theory to ring polymers does not hold since they have no chain ends.

Chain dynamics of ring polymer melts has been extensively investigated in both theoretical[10−14] and experimental[15−31] aspects for the past several decades. In theoretical studies, several interesting models were proposed to express conformations and dynamics of ring molecules; typical examples are double-folded linear conformation[10] or "lattice-animal" conformation[11−13] when their molecular weights (M_w) are large enough to penetrate each other deeply and form a certain entanglement. Alternatively, it is predicted that unentangled rings behave as Rouse chains[14] in relatively smaller M_w region, where the model was created by modifying the simple Rouse model for linear polymers[32] and assuming that they have the Gaussian chain dimensions. In early experimental works on the rheology,[15−19] however, comprehensive results were not obtained owing to a lack of samples with guaranteed ring purity.

Recently, some high-performance liquid chromatography (HPLC) techniques such as interaction chromatography (IC) or liquid chromatography at the critical condition (LCCC) have been developed.[33,34] These methods made it possible to separate rings from linears and to estimate the ring purity accurately. By fully making good use of these methods, truly pure rings were prepared, and several characteristic physical properties were investigated.[23−31,35−37]

As for the rheology, remarkable features were recently reported by Kapnistos et al.[25] They used two kinds of highly-purified ring polystyrene (PS) samples (M_w = 161K and 198K), which have molecular weight significantly larger than the entanglement molecular weight M_e (= 18K for linear PS), and

Received: January 13, 2015
Revised: April 1, 2015
Published: April 20, 2015

DOI: 10.1021/acs.macromol.5b00076
Macromolecules 2015, 48, 3140−3147

revealed that those rings did not exhibit apparent rubbery plateaus but power-law decay of the stress relaxation. These results indicate that rings adopt completely different chain relaxation mechanisms from linears but show some characteristic intermolecular interactions instead. However, only two ring samples in the same molecular weight range were treated in that work, and hence we need to investigate ring chain dynamics covering a wider M_w range.

In this paper, we prepared a series of highly-purified ring polystyrenes with a wider M_w range (10K−240K) and investigated their rheological properties. To discuss the chain relaxation mechanisms of ring chains, the dynamic moduli of the rings obtained were compared with some theoretical models such as the Rouse ring model and the lattice-animal model. Moreover, two characteristic rheological parameters, zero-shear viscosities η_0, and the steady-state recoverable compliance J_e were estimated from the master curves, and their M_w dependence was discussed.

EXPERIMENTAL SECTION

Synthesis, purification, and characterization of a series of ring polystyrene (PS) samples were carried out in the same ways as reported previously.[38] All the six telechelic PSs, whose molecular weights covering the range 10K ≤ M_w ≤ 240K, were anionically synthesized and cyclized by end-to-end ring closure reactions in dilute THF solutions. The purification of ring polymers was carried out by multistep SEC and interaction chromatography (IC) fractionations. Their weight-average molecular weights M_w and molecular weight distribution M_w/M_n were determined by the multiangle light scattering (MALS) and SEC measurements, respectively. The purity of ring samples was evaluated from IC measurements by estimating the peak area ratio between ring and linear chains in the samples. The details of these measurements were described in a previous paper.[36] Their characteristics are summarized in Table 1. As the reference samples for the rheological measurements, nine linear PSs whose M_w ranged from 10K to 240K, six of them are the precursors for ring polymers, were prepared by anionic polymerizations and one with the largest M_w (420K) was purchased from Tosoh Co. Their characteristics are summarized in Table S1 of the Supporting Information. They all show narrow molecular weight distribution (M_w/M_n < 1.05).

Table 1. Molecular Characteristics of a Series of Ring Polystyrene Samples

sample	$M_w \times 10^{-3}$ [a]	M_w/M_n [b]	purity[c]
R-10	12.3	1.05	99.6
R-20	18.4	1.05	99.6
R-40	41.7	1.02	99.7
R-60	59.8	1.02	99.9
R-90	93.0	1.02	99.5
R-240	244	1.02	99.6

[a]Estimated from MALS. [b]Estimated from SEC. [c]Estimated from IC.

Linear dynamic viscoelasticities were measured by using the ARES-G2 rheometer (TA Instruments) with 8 mm diameter and 0.1 rad cone angle cone plates. Temperatures for measurements were varied in the range of 120−195 °C for ring samples under the nitrogen environment to prevent the chain degradations, and the highest temperature was varied depending on the molecular weight of the samples. The measurement frequency range was 0.1−100 s^{-1} in a linear strain region of 5%. Samples for rheological measurements were prepared by a hot-pressing into a disk of 8 mm diameter at 150 °C for less than 5 min in the air and subsequently annealed in a vacuum oven at 180 °C for 24 h in order to remove any air bubbles. Master curves of the dynamic storage and loss moduli, $G'(\omega)$ and $G''(\omega)$, were constructed by applying the time−temperature superposition (TTS) principle[39] with the reference temperature T_{ref} of 160 °C. Specifically, the experimental data obtained at each temperature were vertically shifted by $b_T = \rho(T_{ref})T_{ref}/\rho(T)T$, where $\rho(T)$ is the density for PS following $\rho(T) = 1.2503-6.05 \times 10^{-4}T$.[40] Subsequently, the data were horizontally shifted by a_T to achieve the best fitting. After the rheological measurements, all the ring samples were tested by SEC and IC to check whether the chain degradations occurred by heating and shearing.

RESULTS AND DISCUSSION

Molecular characteristics of six ring polystyrene (PS) samples are summarized in Table 1. An example of multistep fractionation process of the original ring product was described in a previous paper.[41] All the final products of rings were confirmed by IC measurements to have ultrahigh purity over 99.5%. Note that the purity of rings was determined from the peak area ratio between ring and linear chains in the ring samples and that the experimental errors of the purity are less than 0.1%. As an example, IC chromatograms for L-240 and R-240 are shown in Figures 1a and 1b, respectively. Two peaks for the linear (eluted at around 4.5−6 min) and the ring (6−8 min) were perfectly separated due to the difference in the chain architecture. We can rigorously estimate that the purity of this ring is 99.6%. We regard that the ring samples in this study are as pure as possible at present. Furthermore, since all the cyclization reactions of telechelic PSs were performed in a good solvent (THF) for PS, the fractions of knotted ring products must be negligibly small in all the ring samples, even for the largest M_w ring, R-240, by referring to the previous report.[42]

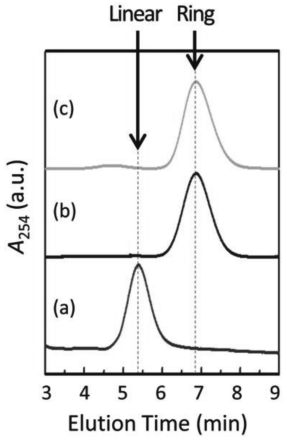

Figure 1. IC chromatograms of (a) L-240 and (b) R-240 before rheological measurements, and (c) R-240 after the measurements.

Figure 2 shows the angular frequency ω dependence of the storage and loss moduli, $G'(\omega)$ and $G''(\omega)$, for six ring PSs, (a) R-10, (b) R-20, (c) R-40, (d) R-60, (e) R-90 and (f) R-240, compared with their linear counterparts. Master curves of the samples were constructed by shifting the experimental data obtained at each temperature. It is clear from Figure 2 that each ring PS shows remarkably faster terminal relaxation compared to its linear counterpart within the entire M_w range examined in this study. Moreover, linear PSs exhibit clear rubbery plateaus when their M_w are larger than the critical entanglement molecular weight M_c (= $2M_e$ = 36K), while rings revealed no rubbery plateaus even though their M_w are sufficiently larger than M_c for linear PSs. These data strongly suggest that ring chains form little intermolecular entanglements in bulk and that they reveal completely different chain relaxation mechanisms

DOI: 10.1021/acs.macromol.5b00076
Macromolecules 2015, 48, 3140−3147

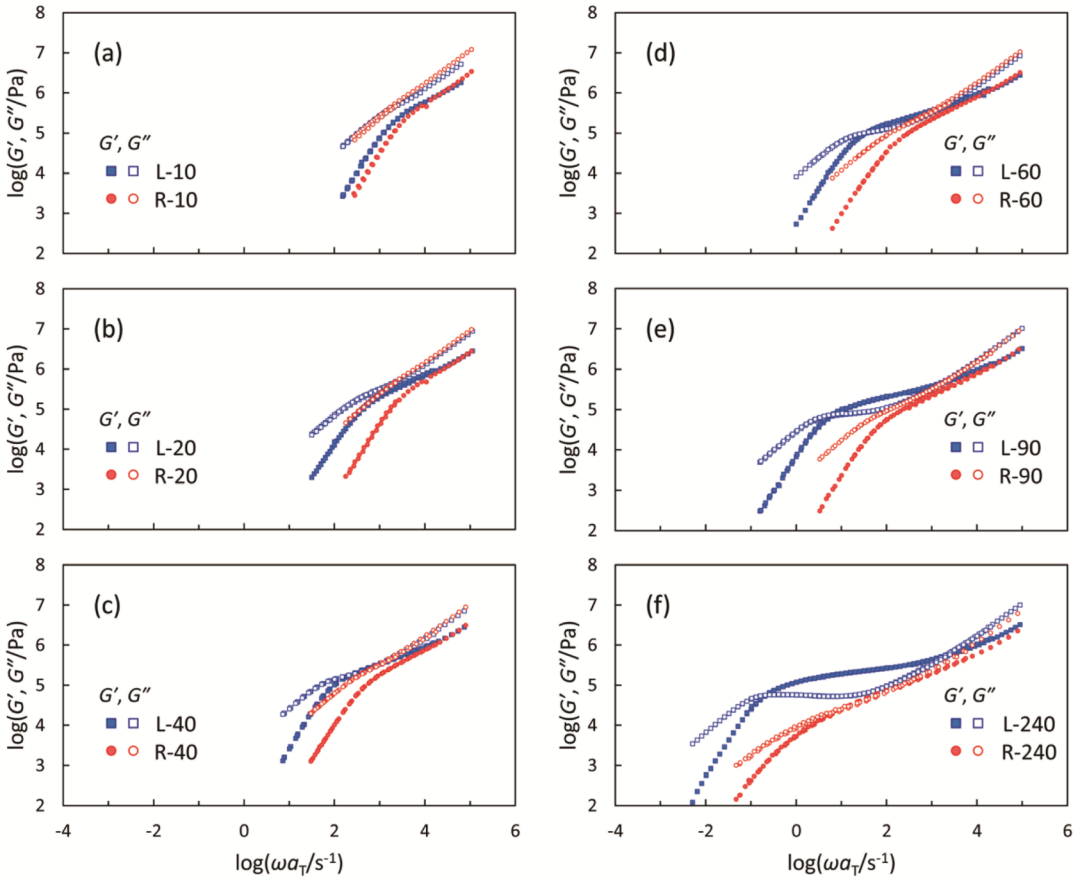

Figure 2. Master curves of G' (closed) and G'' (open) for ring PSs (red circle) compared with those for the linear counterparts (blue square) at T_{ref} = 160 °C: (a) R-10, (b) R-20, (c) R-40, (d) R-60, (e) R-90 and (f) R-240.

from linear ones. In particular, the largest ring R-240 exhibits the power-law moduli decay with a slope of nearly 0.5 in 3 decades of ω, instead of the plateau. These results agree well with the recent reports of Vlassopoulos et al.[25,29] Moreover, both linear and ring PSs, except for R-240, exhibit typical moduli decay of $G' \sim \omega^2$ and $G'' \sim \omega^1$ in the terminal region. On the other hand, for R-240, an evident terminal relaxation behavior was not observed, since the rheological measurement was stopped at 195 °C to minimize the chain degradations.

After rheological measurements, all the rings were confirmed to show very little chain degradations by IC measurements. As an example, an IC chromatogram for R-240 after rheological measurements is shown in Figure 1c. This figure shows the existence of a tiny amount of linear byproducts, which is eluted at around 4.5−6 min, and the amount was approximately 5% through the measurements. However, the main peak of the ring keeps the sharp shape as that before the measurement as shown in Figure 1b. In the same way, R-90 shows a small peak (less than 5%) of the linear byproducts, while other ring samples (R-60 to R-10) reveal almost no signal for the chain degradations after the rheological measurements. Unfortunately, we cannot accurately judge when the chain degradations occur during the rheological measurements and how the linear byproducts affect the rheological response of ring polymers. We are currently investigating that by purposely blending the linears into the rings in the same way as Kapnistos et al.[25] The results of the blending will be reported in another paper in the near future. In any case, it is convinced that we investigated the rheological behavior of highly-purified ring polymers as exactly as possible at present.

Figures 3a and 3b show the temperature T dependence of the horizontal shift factors a_T for linear and ring PSs, respectively. Linear PSs with higher M_w (>40K) exhibited a common T dependence as represented by the solid curve; log $a_T = -c_1(T - T_{ref})/(c_2 + T - T_{ref})$ with T_{ref} = 433 K, c_1 = 6.3 and c_2 = 110 K. For linear PSs with lower M_w (≤40K), the correction was needed since they show lower glass transition temperatures T_g depending on their molecular weights. On the other hand, T dependence of a_T for ring PSs is apparently independent of their molecular weights and similar to that for long linear ones as shown in Figure 3b. This result implies that a_T for ring PSs are not necessary to correct, and namely T_gs of ring PSs in this study are practically the same as those of long linear PSs, although we were not able to obtain the accurate T_g values for ring PSs in this study due to the limitation of the amount of the samples. The previous reports also support our suggestion of the equivalence of T_g for rings.[23,28] Strictly speaking, however, small deviations for the largest ring (R-240) as well as the smaller rings (R-10 and R-20) were recognized when we attain the best fitting of the data at each temperature. This is probably related to the difference of the local chain conformation and also the viscoelastic segment size of the ring chains. The details are discussed later.

Moreover, we should carefully treat the dynamic moduli in high ω region ($\omega > 10^4$ s^{-1}) in Figure 2. Four rings with relatively small M_w (R-10 to R-60) exhibit slightly higher G'' compared to their linear counterparts, while the moduli for the

DOI: 10.1021/acs.macromol.5b00076
Macromolecules 2015, 48, 3140−3147

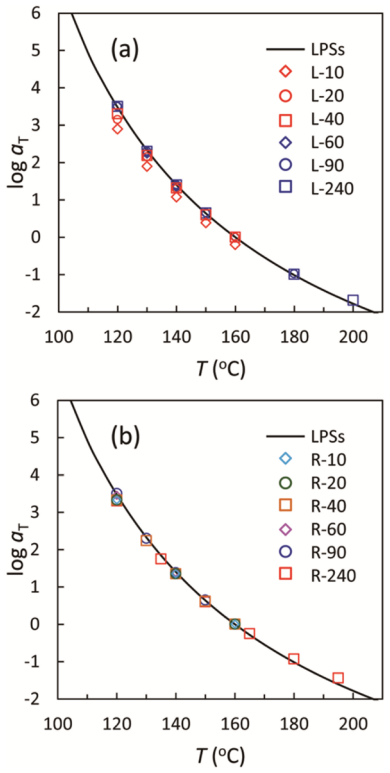

Figure 3. Temperature dependence of the horizontal shift factors a_T for (a) linear and (b) ring PSs. The solid curves indicate the T dependence of a_T for long linear PSs (M_w > 40K).

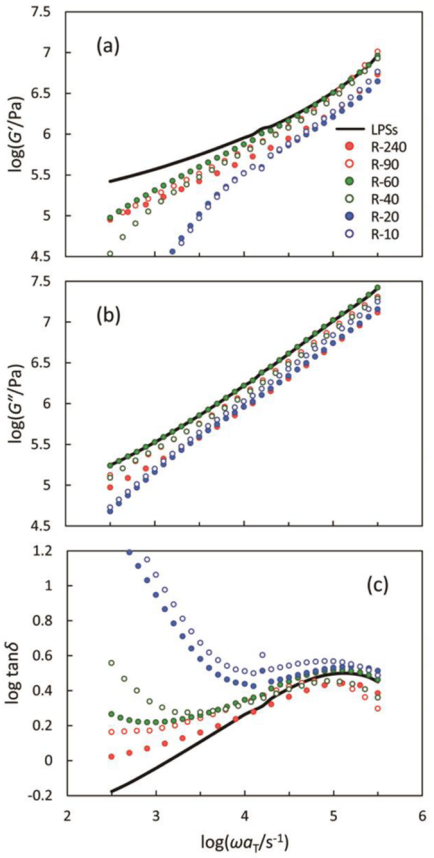

Figure 4. (a) G', (b) G'' and (c) tan δ for ring PSs measured at 120 °C and horizontally shifted by the constant a_T values for long linear PSs (a_T = 3.5).

largest ring R-240 in high ω are rather smaller than those for L-240. This result is thought to reflect the differences in the local chain conformation between ring and linear molecules, which could be directly correlated with the viscoelastic segment size. In order to discuss this issue in more detail, the data of G', G'', and the loss tangents (tan δ) for ring PSs measured at 120 °C were put together in Figure 4a–c, since the data at this temperature most strongly reflect the effect of glass transition in this study. Note that all the data in Figure 4a–c were horizontally shifted by the constant a_T values for long linear PSs (a_T = 3.5), and hence they are essentially the same as the raw data. The corresponding data for linear PSs are shown in Figure S1 of the Supporting Information. First, from Figure 4c, the peak top positions of all the rings are similar to those of long linear PSs at around $\omega = 10^5$ s^{-1} in contrast to those of shorter linear PSs. This result indicates that the ring samples in this study actually have similar T_g values to the long linear PSs, as mentioned above. In addition, it is clear from Figures 4a and 4b that the dynamic moduli of rings in high ω region are exhibiting the following feature depending on their molecular weight; the largest ring (R-240) as well as the smaller rings (R-10 and R-20) has obviously lower moduli compared to the rings with the mediate M_w (R-40 to R-90) and linear PSs, even though all the rings have the similar T_g values. This result may suggest that both large and small rings reveal deviations from the Gaussian chain conformation. Actually, there is no necessity for ring polymers to have the Gaussian chain conformation in whole M_w range due to the absence of the chain end. We are currently confirming this non-Gaussian behavior of both large and small rings in bulk by small-angle neutron scattering (SANS) measurements. This result will be reported in the near future.

To examine the relaxation mechanisms of ring polymers, we apply two polymer dynamics models, i.e., one is the Rouse ring model[14] and the other is the lattice-animal model,[11−13] to the experimental dynamic moduli for ring PSs. First, the Rouse ring prediction was performed. The predicted curves of the Rouse ring chains can be expressed by the following equations:

$$G'(\omega) = \frac{2\rho RT}{M_w} \sum_{p\geq 1} \frac{\omega^2 {\tau_p}^2}{1 + \omega^2 {\tau_p}^2} \quad (1)$$

$$G''(\omega) = \frac{2\rho RT}{M_w} \sum_{p\geq 1} \frac{\omega \tau_p}{1 + \omega^2 {\tau_p}^2} + 10^{1.85}\omega \quad (2)$$

$$\tau_p = \frac{\tau_{ring}}{p^2}, \quad \tau_{ring}(M_w) = \frac{\tau_{linear}(M_w)}{4} \ (\propto {M_w}^2) \quad (3)$$

where ρ is the density of polystyrene, R is the gas constant, p is the mode number, and τ_p is the pth Rouse relaxation time. We consider the contribution from the glassy mode of G'' ($G''_{glass} = 10^{1.85}\omega$) in eq 2 to discuss their dynamic behavior in a wider frequency range. We actually treated the data up to $\omega = 10^4$ s^{-1} because the glassy mode of G' can be neglected within this region. The longest Rouse relaxation time of ring chains, τ_{ring}, in eq 3 is defined as a quarter of that of the Rouse linear chains τ_{linear} with the same M_w.[14] We evaluated τ_{ring} from $\langle\tau\rangle_w$ for the Rouse linear PSs. Here, $\langle\tau\rangle_w$ for L-20 (= 2.0×10^{-3} s) was used as a reference value, and each τ_{ring} was estimated from eq 3, since L-20 sample should not show intermolecular entanglements and behave as a simple Rouse linear chain. The results of

DOI: 10.1021/acs.macromol.5b00076
Macromolecules 2015, 48, 3140−3147

the Rouse ring fitting are shown in Figure 5. Among them, the experimental data for R-40 agree well with the calculated

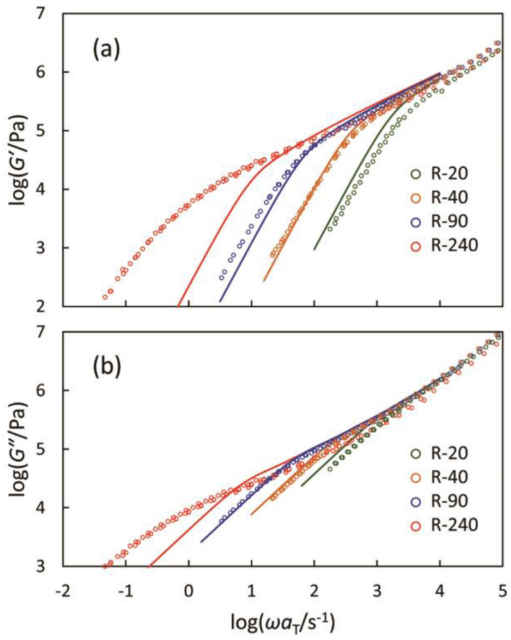

Figure 5. Rouse ring model prediction curves (solid lines) of (a) G' and (b) G'' for R-20, R-40, R-90, and R-240, compared with the experimental data (open circles) at T_{ref} = 160 °C.

curves, although they still have small deviations. This result strongly suggests that ring molecules around this molecular weight behave like Rouse ring chains, which have the Gaussian ring chain conformation, although there is no necessity that they have the Gaussian chain distribution. On the other hand, other ring samples exhibit a clear deviation from the predicted curves, especially in the terminal region. The experimental data for R-90 reveal slightly slower terminal relaxation than the calculated curves, while R-240 exhibit tremendous relaxation delay compared to the Rouse ring prediction. Actually, the experimental $\langle\tau\rangle_w$ for R-240 is more than 30 times larger than that for the predicted Rouse ring. From these results, we can interpret that R-90 exhibits some small intermolecular interactions and that R-240 adopts well-entangled state, although their chain relaxation mechanisms must be totally different from those for linear chains. To the contrary, the smaller ring, R-20, shows an apparently faster terminal relaxation compared to the Rouse ring prediction in Figure 5. This difference might be originated from the non-Gaussianity of the small rings' conformation, which induces a change of the viscoelastic segment size.

To examine the relaxation mechanisms of relatively higher M_w rings, R-90 and R-240, the lattice-animal model prediction was subsequently performed. The predicted stress relaxation modulus $G(t)$ for rings is given by the equation

$$G(t) = \frac{\rho RT}{M_e}\left(\frac{t}{\tau_e}\right)^{-2/5} \exp\left(-\frac{t}{\tau_{ring}}\right) + 10^{1.85}t^{-1} \quad (4)$$

where t is the inverse of frequency ($= 1/\omega$), τ_e is the relaxation time for an entangled strand (τ_e = 0.002 s), and τ_{ring} is the relaxation time for rings expressed by $\tau_{ring} = \tau_e(N/N_e)^{5/2}$. The details are described in other papers.[11−13,25,29] The glassy mode ($G_{glass} = 10^{1.85}t^{-1}$) was added in eq 4, which is directly corresponding to eq 2. Owing to the complexity of eq 4, we treat the data as a function of t, i.e., the experimental stress relaxation moduli $G(t)$ were obtained from the Fourier transformation of G' and G''. The predicted results of $G(t)$ for R-90 and R-240 in this model are shown in Figure 6, together with the experimental data and the Rouse ring predictions.

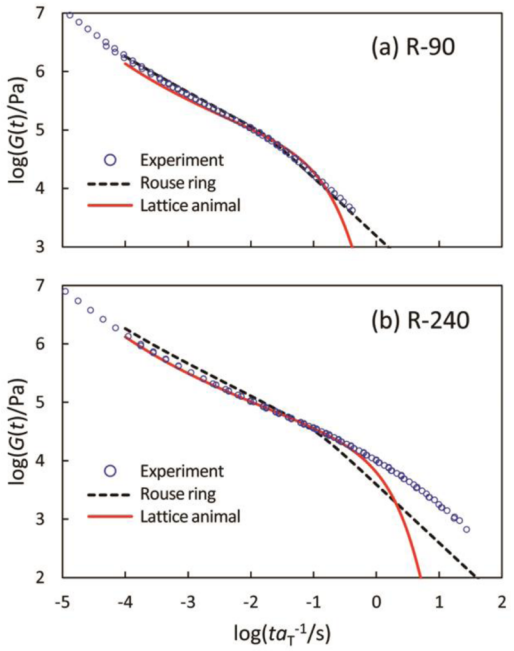

Figure 6. Lattice-animal model prediction curves (red solid line) of the stress relaxation moduli $G(t)$ for (a) R-90 and (b) R-240, compared with the experimental data (blue circle) and Rouse ring prediction curves (black dashed line) at T_{ref} = 160 °C.

Two differences are clearly observed in the short ($t < 10^{-2}$ s) and long t ($t > 10^{-2}$ s) region in Figure 6. In the short t region, the modulus of the lattice-animal model is specifically lower than that of the Rouse ring, reflecting the difference in the local chain conformation. In long t, the terminal relaxation behavior between them is evidently different, i.e., in the Rouse ring model, $G(t)$ relaxes as a function of t^{-1}, while $G(t)$ decreases exponentially with t in the lattice-animal model. As mentioned above, the experimental data of R-90 agree with the Rouse ring model well. On the other hand, $G(t)$ for R-240 agrees with the lattice-animal model much better than the other in relatively shorter t region ($t < 10^{-1}$ s), allowing low values of the modulus at $10^{-5} < t < 10^{-3}$ s and the power law relaxation with a slope of 0.5 at $10^{-3} < t < 10^{-1}$ s, while the terminal relaxation behavior ($t > 10^{-1}$ s) does not agree with the model predictions in the same way as the previous works.[25,29] Although we do not know how a little linear contamination affects their rheological behavior, this result strongly suggests that some intermolecular interactions such as ring penetration occurred for the large ring, R-240. To verify the effect of the intermolecular interactions, the development of the models and simulations is greatly desired.

The relaxation mechanisms of ring chains were examined from the viewpoints of M_w dependence of rheological parameters, the zero-shear viscosities, η_0, and the steady state recoverable compliances, J_e. These two parameters, where both

DOI: 10.1021/acs.macromol.5b00076
Macromolecules 2015, 48, 3140−3147

reflect the characteristic relaxation behavior in the terminal region, are represented by the following equations:

$$\eta_0 = \lim_{\omega \to 0} G''(\omega)/\omega \quad (5)$$

$$J_e = (1/\eta_0^2) \lim_{\omega \to 0} (G'(\omega)/\omega^2) \quad (6)$$

These two parameters for all the samples at T_{ref} = 160 °C were estimated in two ways. First, they were estimated from the limiting values by following eqs 5 and 6, as shown in Figure S2 of the Supporting Information. Second, they were estimated directly from the master curves of the terminal region in Figure 2 by extrapolating the approximate straight lines with slopes of 2 and 1 in G' and G'', respectively, as shown in Figure S3 of the Supporting Information. In these two ways, the values obtained were almost the same, and they are summarized in Table 2.

Table 2. Rheological Parameters, η_0 and J_e, for Ring Polystyrenes at T_{ref} = 160 °C

samples	$\eta_0 \times 10^{-3}$ (Pa·s)	$J_e \times 10^5$ (Pa^{-1})
R-10	0.246 ± 0.038	0.053 ± 0.015
R-20	0.261 ± 0.017	0.083 ± 0.022
R-40	0.643 ± 0.040	0.32 ± 0.065
R-60	1.19 ± 0.015	0.72 ± 0.080
R-90	1.73 ± 0.075	0.88 ± 0.123
R-240	17.9 ± 2.25	12.1 ± 3.24

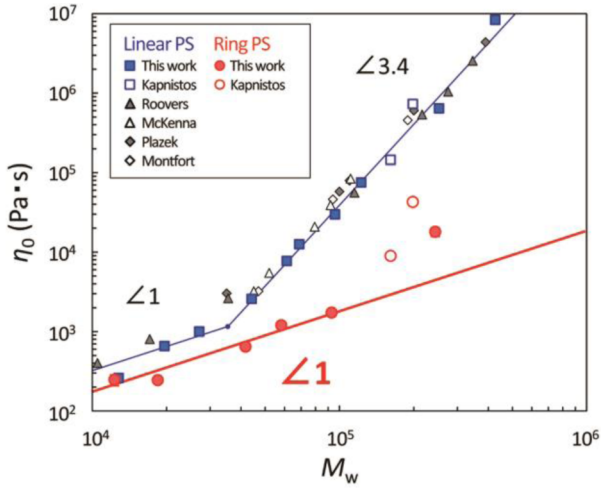

Figure 7. M_w dependence of η_0 for ring PSs compared with linear PSs at T_{ref} = 160 °C. Rings: this study (red closed circle) and Kapnistos et al.[24] (red open circle). Linears: this study (blue closed square), Kapnistos et al.[24] (blue open square), Roovers et al.[18] (black closed triangle), McKenna et al.[19] (black open triangle), Plazek et al.[43] (black closed diamond), and Montfort et al.[44] (black open diamond). The solid and dashed lines are guides for the eyes.

Figure 7 represents the M_w dependence of η_0 for ring PSs compared to the linear ones. The data for two Kapnistos' ring PSs[25] and other linear PSs reported by Roovers et al.,[18] McKenna et al.,[19] Kapnistos et al.,[25] Plazek et al.,[43] and Montfort et al.[44] were also added to this figure after considering the difference of the reference temperature. From this figure, all rings exhibit obviously lower viscosities compared to the linear counterparts in the entire M_w region. Moreover, rings show a clearly different M_w dependence from linears, i.e., η_0 for rings increases simply proportional to molecular weight, i.e., $\eta_0 \sim M_w^{1.0}$ for M_w up to 90K, which is approximately 5 times larger than the entanglement molecular weight M_e (= 18K for linear PS). This result suggests that ring PSs whose M_w are smaller than $5M_e$ apparently show the M_w dependence of η_0 predicted by the Rouse ring chain. On the other hand, when M_w is larger than 90K, it shows a drastic deviation from the dependence of the Rouse-like mode. Actually, R-240 exhibits almost ten times larger η_0 values than the Rouse prediction. When two points of R-90 and R-240 are connected by a straight line, its slope is 2.4 ± 0.1. The lattice-animal model[11,12] predicts $\eta_0 \sim M_w^{3/2}$, while the recent loopy globule model[13] predicts $\eta_0 \sim M_w^{5/3}$. This result also suggests that some intermolecular interactions were generated for the higher M_w ring, as we have already mentioned above. Moreover, R-240 in this study revealed a clearly lower η_0 than the larger Kapnistos ring, R-191, even though our ring has a rather larger M_w. We believe that this result may be deeply related to the actual ring purity.

Furthermore, we universally compare the viscosity data of our rings with other previous experimental results,[23,26,27,29] including different polymer species (1,4-polyisoprene (PI) and poly(ethylene oxide) (PEO)) in the same manner adopted by Pasquino et al.;[29] i.e., the ratios of the zero shear viscosities of the linear $\eta_{0,linear}$ and ring $\eta_{0,ring}$ with the same M_w were plotted as a function of the number of entanglements M_w/M_e. The details were described in ref 29, and the results are shown in Figure 8. In low M_w/M_e (<2) region, all the data including ours

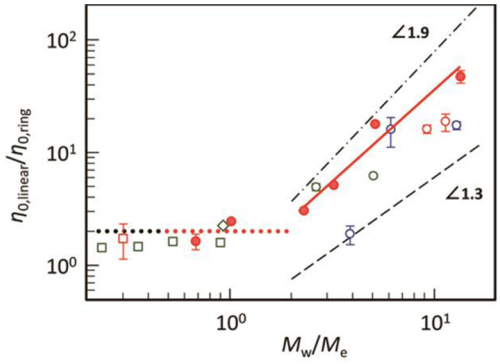

Figure 8. Ratio of η_0 for linear and ring polymers as a function of the number of entanglement M_w/M_e. Symbols are the experimental data for PS (red), PI (blue), and PEO (green), and lines are guides for the eyes. Data in this study (red closed circle) and reported by Pasquino et al.[29] (open circles with each color), Santangelo et al.[23] (red open square), Nam et al.[26] (green open square), and Bras et al.[27] (green open diamond).

exhibit a constant $\eta_{0,linear}/\eta_{0,ring}$ value of approximately 2, which suggest rings in this region show the Rouse ring-like behavior although the master curve for R-20 does not agree with the Rouse prediction. To the contrary, in the high M_w/M_e region (>2), the divergence of the data is observed within the two limiting lines, where the slopes of upper and lower lines are 1.9 and 1.3, respectively. These two values are predicted from the scaling theories for linear and ring chains; i.e., the upper limit 1.9 is assumed when the linear chains follow the improved reptation model[8,9] (the exponent is 3.4), and the rings accept the lattice-animal model[11,12] (1.5), while the lower limit 1.3 is assumed when the linears follow the primary reptation model[6,7] (3.0) and rings follow the loopy globule model[13] (1.7). When we connect our four plots linearly in $M_w/M_e > 2$ as shown as the red line in Figure 8, its slope is 1.6 ± 0.2, which is clearly

DOI: 10.1021/acs.macromol.5b00076
Macromolecules 2015, 48, 3140−3147

larger than the previous work (the slope is 1.2 ± 0.3) by Pasquino et al. This result suggests that our rings have comparatively lower viscosities, which may be related to the actual purity of ring polymers. In addition, our data of four rings are much closer to the upper line in Figure 8. This result also implies that our rings have much higher purity than others. Although we are not able to discuss the picture of chain relaxation mechanism of rings merely from the exponent of the ratio of the viscosities $\eta_{0,linear}/\eta_{0,ring}$, the above facts are meaningful to guarantee the accuracy of our measurements. To quantitatively clarify the mechanisms of rings, more experimental data including much larger rings ($M_w/M_e > 20$) and the further developments of the models and simulations are greatly required.

Figure 9 shows the M_w dependence of the compliances J_e for ring PSs compared to linear ones. Concerning linear molecules,

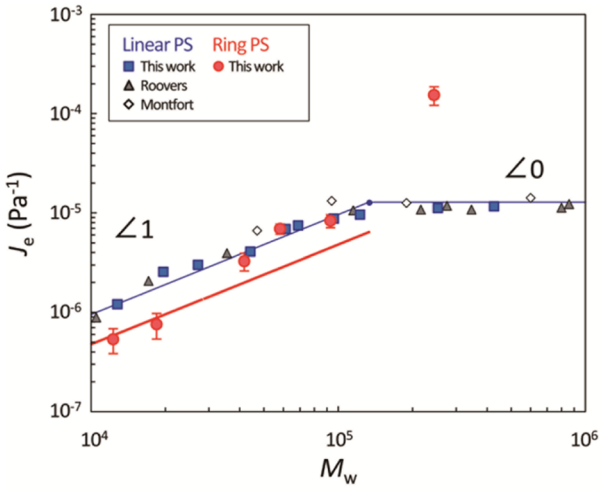

Figure 9. M_w dependence of J_e for ring PSs compared to linear PSs at T_{ref} = 160 °C. The symbols are corresponding to those in Figure 7. The solid and dashed lines are guides for the eyes.

J_e increase in proportional to the increase of M_w ($J_e \propto M_w^{1.0}$) up to $6M_e$, whereas they have a constant value ($J_e \sim 1.2 \times 10^{-5}$ Pa^{-1}) at above $6M_e$. To the contrary, rings apparently show different behavior from linears. Their dependence can be divided into three parts. (i) In a small M_w region ($M_w \leq 20$K), rings have approximately half J_e values of the linear counterparts. (ii) In an intermediate region (40K $\leq M_w \leq$ 90K), they show similar J_e values to the linear ones. (iii) In a larger M_w (90K $< M_w$) region, it shows an obviously higher J_e value. In the Rouse ring prediction, J_e for rings should be a half of that for linears ($J_{e,ring} = J_{e,linear}/2$ with the same M_w). As for the smaller rings ($M_w \leq 20$K), their η_0 and J_e are consistent with the Rouse ring model, while their dynamic moduli do not agree with the model. The reason for this inconsistency is not known at present, and we need further experiments and considerations. However, this may be related to the difference in the local chain conformation of the small rings. In the same way, the master curves for intermediate rings (40K $\leq M_w \leq$ 90K) are apparently similar to those for Rouse rings. However, J_e values for these rings are actually double of the Rouse rings, which is inconsistent with the model. This result may suggest the imperfection of the original model. The largest ring, R-240, exhibits almost 10 times larger J_e than that for the linear counterpart, L-240, indicating that the large ring is moving approximately 10 times more cooperatively than the linear counterpart with the same molecular weight in the terminal relaxation. This deviation is similar to the long branched polymers and can be explained with the lattice-animal conformation of ring polymers.[11−13]

CONCLUSION

We investigated the melt rheology of a series of ring polystyrenes (10K $\leq M_w \leq$ 240K) with ultrahigh purity over 99.5%. They revealed no obvious rubbery plateau and faster terminal relaxation than the linear counterparts in the whole M_w range. The relaxation behavior of ring chains strongly depends on their M_w and is mainly classified into three categories. First, in the smaller M_w ($M_w \leq M_e$) region, the molecular weight dependence of η_0 and J_e for rings is Rouse-like, while the master curves for rings do not agree well with those for the Rouse rings. This disagreement in the master curves is probably related to the difference of the local chain conformation and the viscoelastic segment size. To solve this inconsistency, further experiments, including both conformational and dynamic aspects, are required. Second, the ring chains with the moderate M_w (approximately $2M_e \leq M_w \leq 5M_e$ in this study) apparently behave as the Rouse ring chain from the viewpoint of the master curves and η_0, while the compliances J_e are approximately double of the model. This is probably related to the relaxation mode distribution due to the existence of the small amount of linear contaminations or the imperfection of the original model. Finally, in the larger M_w ($5M_e < M_w$) region, the ring shows an obvious viscosity enhancement as well as a larger J_e value. This result strongly suggests that this large ring generates some intermolecular interactions such as ring penetrations. To quantitatively clarify these interactions, more experimental data and the further development of the theoretical and simulation studies are greatly desired.

ASSOCIATED CONTENT

Supporting Information

Figures S1−S3 and Table S1. This material is available free of charge via the Internet at http://pubs.acs.org.

AUTHOR INFORMATION

Corresponding Authors

*Ph +81-52-789-3211; Fax +81-52-789-3210; e-mail atakano@apchem.nagoya-u.ac.jp (A.T.).
*e-mail yushu@apchem.nagoya-u.ac.jp (Y.M.).

Notes

The authors declare no competing financial interest.

ACKNOWLEDGMENTS

This work was supported in part by a Grant-in-Aid for Scientific Research (No. 24350056) from the Ministry of Education, Science and Culture (MEXT), Japan. This work was also supported partly by the Collaborative Research Program of Institute for Chemical Research, Kyoto University (Grant No. 2013-45), and A.T. is grateful for the support. Authors also acknowledge for the financial support from Global 30 international program and the Program for Leading Graduate Schools at Nagoya University entitled "Integrate Graduate Education and Research Program in Green Natural Sciences".

DOI: 10.1021/acs.macromol.5b00076
Macromolecules 2015, 48, 3140−3147

REFERENCES

(1) Kramers, H. A. *J. Chem. Phys.* **1946**, *14*, 415−424.
(2) Zimm, B. H.; Stockmayer, W. H. *J. Chem. Phys.* **1949**, *17*, 1301−1314.
(3) Casassa, E. F. *J. Polym. Sci., Part A* **1965**, *3*, 605−614.
(4) Roovers, J.; Toporowski, P. M. *Macromolecules* **1983**, *16*, 843−849.
(5) McLeish, T. C. B. *Science* **2002**, *297*, 2005−2006.
(6) de Gennes, P. G. *Scaling Concept in Polymer Physics*; Cornell University Press: Ithaca, NY, 1979.
(7) Doi, M.; Edward, S. E. *The Theory of Polymer Dynamics*; Clarendon: Oxford, UK, 1986.
(8) Watanabe, H. *Prog. Polym. Sci.* **1999**, *24*, 1253−1403.
(9) McLeish, T. C. B. *Adv. Phys.* **2002**, *51*, 1379−1527.
(10) Klein, J. *Macromolecules* **1986**, *19*, 105−118.
(11) Rubinstein, M. *Phys. Rev. Lett.* **1986**, *24*, 3023−3026.
(12) Obukhov, S. P.; Rubinstein, M.; Duke, T. *Phys. Rev. Lett.* **1994**, *73*, 1263−1266.
(13) Milner, S. T.; Newhall, J. D. *Phys. Rev. Lett.* **2010**, *105*, 208302.
(14) Watanabe, H.; Inoue, T.; Matsumiya, Y. *Macromolecules* **2006**, *39*, 5419−5426.
(15) Roovers, J. *Macromolecules* **1985**, *18*, 1359−1361.
(16) McKenna, G. B.; Hadziioannou, G.; Lutz, P.; Hild, G.; Strazielle, C.; Straupe, C.; Remmp, P.; Kovacs, A. J. *Macromolecules* **1987**, *20*, 498−512.
(17) Orrah, D. J.; Semlyen, J. A.; Ross-Murphy, S. B. *Polymer* **1988**, *29*, 1452−1454.
(18) Roovers, J. *Macromolecules* **1988**, *21*, 1517−1521.
(19) McKenna, G. B.; Hostetter, B. J.; Hadjichristidis, N.; Fetters, L. J.; Plazek, D. J. *Macromolecules* **1989**, *22*, 1834−1521.
(20) Mills, P. J.; Mayer, J. W.; Kramer, E. J.; Hadziioannou, G.; Lutz, P.; Stazielle, C.; Rempp, P.; Kovacs, A. J. *Macromolecules* **1987**, *20*, 513−518.
(21) Orrah, D. J.; Semlyen, J. A.; Ross-Murphy, S. B. *Polymer* **1988**, *29*, 1455−1458.
(22) Tead, S. F.; Kramer, E. J.; Hadziioannou, G.; Antonietti, M.; Sillescu, H.; Lutz, P.; Stazielle, C. *Macromolecules* **1992**, *25*, 3942−3947.
(23) Santangelo, P. G.; Roland, C. M.; Chang, T.; Cho, D.; Roovers, J. *Macromolecules* **2001**, *34*, 9002−9005.
(24) Kawaguchi, D.; Masuoka, K.; Takano, A.; Tanaka, K.; Nagamura, T.; Torikai, N.; Dalgliesh, R. M.; Langridge, S.; Matsushita, Y. *Macromolecules* **2006**, *39*, 5180−5182.
(25) Kapnistos, M.; Lang, M.; Vlassopoulos, D.; Pyckhout-Hintzen, W.; Richter, D.; Cho, D.; Chang, T.; Rubinstein, M. *Nat. Mater.* **2008**, *7*, 997−1002.
(26) Nam, S.; Leisen, J.; Breedveld, V.; Beckham, H. W. *Polymer* **2008**, *49*, 5467−5473.
(27) Bras, A. R.; Pasquino, R.; Koukoulas, T.; Tsolou, G.; Holderer, O.; Radulescu, A.; Allgaier, J.; Mavrantzas, V. G.; Pyckhout-Hintzen, W.; Wischnewski, A.; Vlassopoulos, D.; Richter, D. *Soft Matter* **2011**, *7*, 11169−11176.
(28) Kawaguchi, D.; Ohta, Y.; Takano, A.; Matsushita, Y. *Macromolecules* **2012**, *45*, 6748−6752.
(29) Pasquino, R.; Vasilakopoulos, T. C.; Jeong, Y. C.; Lee, H.; Rogers, S.; Sakellariou, G.; Allgaier, J.; Takano, A.; Bras, A. R.; Chang, T.; Gooβen, S.; Pyckhout-Hintzen, W.; Wischnewski, A.; Hadjichristidis, N.; Richter, D.; Rubinstein, M.; Vlassopoulos, D. *ACS Macro Lett.* **2013**, *2*, 874−878.
(30) Bras, A. R.; Gooβen, S.; Krutyeva, M.; Radulescu, A.; Farago, B.; Allgaier, J.; Pyckhout-Hintzen, W.; Wischnewski, A.; Richter, D. *Soft Matter* **2014**, *10*, 3649−3655.
(31) Gooβen, S.; Bras, A. R.; Krutyeva, M.; Sharp, M.; Falus, P.; Feoktystov, A.; Gasser, U.; Pyckhout-Hintzen, W.; Wischnewski, A.; Richter, D. *Phys. Rev. Lett.* **2014**, *113*, 168302.
(32) Rouse, P. E. *J. Chem. Phys.* **1953**, *21*, 1272−1280.
(33) Pasch, H. Trathnigg, B. *HPLC of Polymers*; Springer: Berlin, 1998.
(34) Lee, H. C.; Lee, H.; Lee, W.; Chang, T.; Roovers, J. *Macromolecules* **2000**, *33*, 8119−8121.
(35) Takano, A.; Kushida, Y.; Ohta, Y.; Masuoka, K.; Matsushita, Y. *Polymer* **2009**, *50*, 1300−1303.
(36) Takano, A.; Ohta, Y.; Masuoka, K.; Matsubara, K.; Nakano, T.; Hieno, A.; Itakura, M.; Takahashi, K.; Kinugasa, S.; Kawaguchi, D.; Takahashi, Y.; Matsushita, Y. *Macromolecules* **2012**, *45*, 369−373.
(37) Gooβen, S.; Bras, A. R.; Pyckhout-Hintzen, W.; Wischnewski, A.; Richter, D.; Rubinstein, M.; Roovers, J.; Lutz, P. J.; Jeong, Y.; Chang, T.; Vlassopoulos, D. *Macromolecules* **2015**, *48*, 1598−1605.
(38) Cho, D.; Masuoka, K.; Koguchi, K.; Asari, T.; Kawaguchi, D.; Takano, A.; Matsushita, Y. *Polym. J.* **2005**, *37*, 506−511.
(39) Ferry, J. D. *Viscoelastic Properties of Polymers*, 3rd ed.; Wiley: New York, 1995.
(40) Zoller, P., Walsh, D., Eds.; *Standard Pressure-Volume-Temperature Data for Polymers*; Technomic Publishing Co.: New York, 1995.
(41) Doi, Y.; Ohta, Y.; Nakamura, M.; Takano, A.; Takahashi, Y.; Matsushita, Y. *Macromolecules* **2013**, *46*, 1075−1081.
(42) Ohta, Y.; Nakamura, M.; Matsushita, Y.; Takano, A. *Polymer* **2012**, *53*, 466−470.
(43) Plazek, D. J.; O'Rourke, V. M. *J. Polym. Sci., Part A-2* **1971**, *9*, 209−243.
(44) Montfort, J. P.; Marin, G.; Monge, P. *Macromolecules* **1984**, *17*, 1551−1560.

DOI: 10.1021/acs.macromol.5b00076
Macromolecules 2015, 48, 3140−3147